Trans. JWRI, Vol. 36, (2007), No. 2

Characteristics of Hot Extruded P/M Aluminum Alloy when Using the Rapidly Solidified Powder SWAP Process†

IMAI Hisashi*, KAWAKAMI Masashi, KONDOH Katsuyoshi***, OTSUKA Isamu**** and IZAKI Hiroshi******

Abstract

The characteristics of hot extruded aluminum alloy when using the rapidly solidified powder Spinning Water Atomization Process (SWAP) have been investigated. SWAP is one of advanced powder processing technologies to prepare high-performance powder particles with fine microstructures. In this study, A7075 aluminum alloy powder were produced by SWAP, and no intermetallic compound was detected in the raw powder. Microstructures and micro-hardness dependence on annealing temperature has been examined. Mechanical properties of the powder metallurgy (P/M) aluminum alloys consolidated by hot extrusion were superior to those of wrought alloys using ingot billets. A7075 wrought P/M alloys via T5 heat treatment show yield stress of 370 MPa and elongation of 15 % at the extrusion temperature of 623 K.

KEY WORDS: (Aluminum alloy) (Spinning Water Atomization Process (SWAP)) (Hot extrusion)

1. Introduction

In general, aluminum alloys are widely used as industrial materials because of their excellent characteristics such as low density, high specific strength, and good electrical and thermal conductivities [1]. A7075 aluminum alloy, which has the highest tensile strength compared to other aluminum alloys, is used as structural components in aircraft, automotives, and hobby goods. More excellent mechanical properties are strongly required for further applications.

The rapid solidification process is effective in forming fine and supersaturated microstructures, and non-equilibrium phases such as amorphous structures, and to increase limits of solubility [2, 3]. Conventional processes by high-pressure gas atomization [4] and water atomization [5, 6] produce rapidly solidified powders with cooling rates of 10^2~10^5 K/s. Spinning Water Atomization Process (SWAP) combined with water atomization and gas atomization, as schematically illustrated in **Fig.1**, produces rapidly solidified powder with a higher cooling rate up to 10^6 K/s and is available to prepare amorphous iron powder with a particle size of 300μm. [7, 8]

In this study, the strengthening behavior of P/M A7075 aluminum alloy produced by SWAP is examined, compared to that of the conventional wrought aluminum alloys when using ingot metallurgy (I/M) billets. The dependence of their microstructures and mechanical properties on the thermal history in extrusion was investigated when applying a T5 heat treatment after hot extrusion. In particular, the effect of the precipitates and their coarsening was examined by X-ray diffraction analysis, optical microscopy and scanning electron microscope observation.

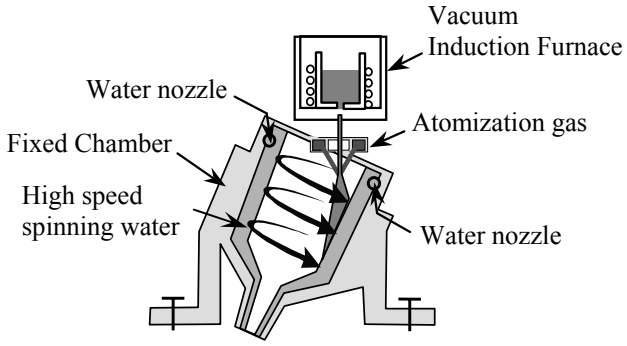

Fig.1 Schematic illustration of Spinning Water Atomization Process (SWAP).

† Received on December 14, 2007
* Specially Appointed Researcher
** Graduate Student
*** Professor
**** EPSON ATMIX CORPORATION
Transactions of JWRI is published by Joining and Welding Research Institute, Osaka University, Ibaraki, Osaka 567-0047, Japan

2. Experimental Procedure

2.1 Raw powder and cold compaction

Table 1 shows the chemical compositions of A7075 raw powder particles from SWAP used in this study. **Figure 2** indicates their morphology observed by scanning electron microscopy (SEM, JSM-6500F: JEOL) and their particle size distribution of A7075 powder measured by particle size distribution analyzer (LA-950: HORIBA) is shown in **Fig.3**. The powder shows different forms including spherical and tear patterns, it is heterogeneous and its mean particle size is 33.84 μm. The thermal behavior due to microstructure changes, in particular the precipitation of supersaturated intermetallics, of the as-received powder during annealing was investigated by differential thermal analysis (DTG-60: SHIMADZU Co.) under a heating rate of 10 K/min in Ar gas atmosphere from room temperature up to 773 K. Intermetallic compounds in the powder and ingot billet were identified by high-temperature X-ray diffraction (XRD-6100: SHIMADZU Co.), operated at 20 kV and 2 mA, and using Cu Kα radiation (λ=1.5406 Å). The XRD patterns were measured between 35 °≦2θ≦45 °at room temperature, and within the range from 573 K to 773 K in every 25 K. The step size of diffraction angle (2θ) and scanning speed were 0.02 °and 4 °/min, respectively. Micro-Vicker's hardness (HMV-2T: SHIMADZU Co.) with loading of 0.49 N was measured on the annealed powder. The microstructural observation by SEM installed with X-ray energy dispersive spectroscopy (EDS EX-64175JMU: JEOL) was carried out on the as-received raw powder. The changes in microstructures were investigated when applying the heat treatment at 623-723 K for 86.4 ks in Ar gas atmosphere. Raw powder was consolidated to prepare green compacts for extruding billets by applying a pressure of 600 MPa at room temperature (2000 kN press (SHP-200-450: SHIBAYAMAKIKAI Co.)). The relative density of the billets was approximately 82 %.

Table 1 Chemical compositions of A7075 powder (wt%).

Si	Fe	Cu	Mn	Mg	Cr	Zn	Ti	Al
0.15	0.20	1.60	0.02	2.48	0.23	5.14	0.03	Bal.

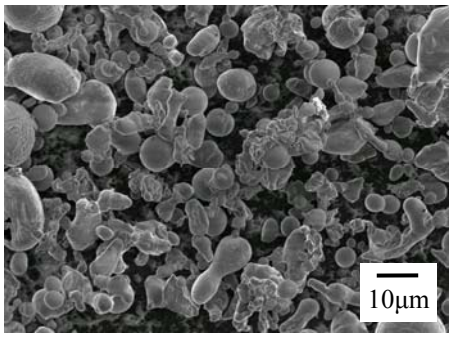

Fig.2 Scanning electron micrograph of SWAP- A7075 powder.

2.2 Hot extrusion

Figure 4 shows a thermo-mechanical treatment conditions of T5 used in hot extrusion. The green compact billets were heated at 623 K, 673 K, and 723 K for 180 s with a heating ratio of 2 K/s in Ar gas atmosphere by the infrared ray gold image furnace (TPC-1000:ULVAC Co.). After heating the billet, it was immediately consolidated to 7mmdiameterrod by hot extrusion. The extrusion ratio and speed was 37.7 and 0.3 mm/s, respectively. After hot extrusion, the wrought material was immediately quenched in a water bath, and then annealed at 393 K for 84.6 ks under the nominal aging of the T6 treatment condition used in A7075 [1]. The same process conditions were also applied when preparing hot extruded alloys using A7075 I/M billets.

2.3 Evaluation on A7075 wrought alloys

Mechanical properties of both P/M and I/M extruded materials were evaluated by using a tensile testing machine (RTC-1310A: ORIENTEC) with a strain rate of 5×10^{-4} s^{-1}. Micro-Vicker's hardness measurement with loading of 0.49 N and microstructural observation by SEM – EDS were carried out on the specimens.

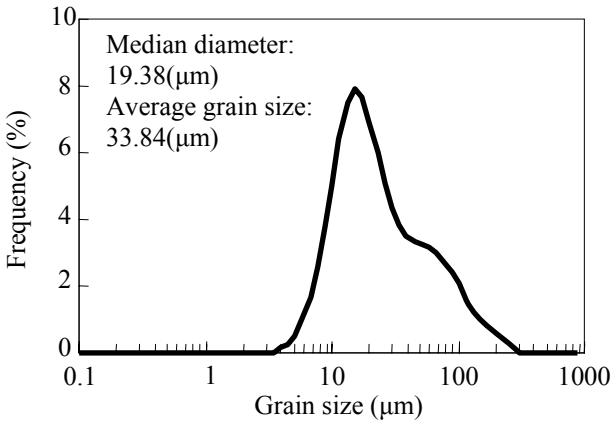

Fig.3 Particle size distribution of A7075 powder.

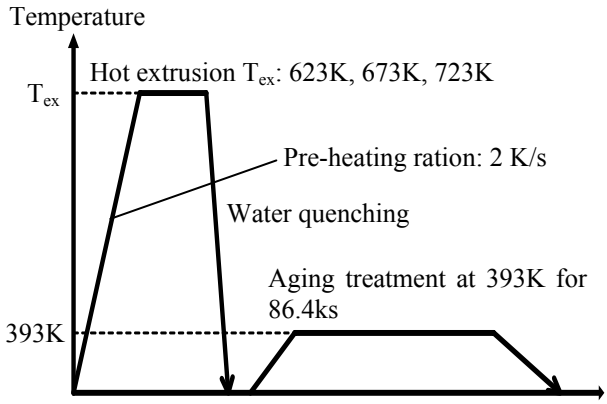

Fig.4 Thermo-mechanical treatment condition of T5 used in hot extrusion.

3. Results and Discussion

3.1 Characteristics of as-received and annealed A7075 powder

Figure 5 shows DTA profiles of A7075 raw powder and ingot billet. Exothermic heats at 503 K and 653 K were detected in A7075 raw powder. This produces some changes of microstructure, in particular precipitation of supersaturated compounds in the matrix by rapid solidification, occur around these temperatures. On the other hand, no exothermic heat or endothermic heat was observed in the ingot billet. Then, the heat treatment on the powder was carried out at the temperature range from 623 K to 723 K in Ar gas atmosphere to evaluate the microstructures changes. **Figure 6** reveals SEM images of as-received A7075 powder (a), and heat-treated ones at various temperatures (b)~(d). For the quantitative evaluation of the grain growth in the A7075 powder during annealing, the image analysis software (4.0J Image Pro Plus) was applied on SEM photos shown in Fig.6. The dependence of the mean grain size calculated by the software on the heat treatment temperature is shown in **Fig.7**. Microstructure observation results indicate that some intermetallic compounds, corresponding to white particles shown in Fig.6, are obviously detected after annealing. Their coarsening also occurs with increases in the heating temperature. On the other hand, Fig.7 indicates that the mean grain size gradually increases by annealing, and the saturated value is 4.5 μm in diameter at 723 K. **Figure 8** shows high-temperature XRD patterns of A7075 powder and ingot billet at various temperatures. Figure 8 (a) indicates that the diffraction angle of the aluminum peak shifts to the lower angle side by annealing the powder, compared to the as-received one. According to Bragg's law ($2d_{hkl}\cdot\sin\theta=n\lambda$, d_{hkl} ; distance between atoms, θ; diffraction angle, λ; X-ray wavelength, n=1,2,3,・・・), the decrease of θ means a reduction of d_{hkl}, that is, decreases of the lattice parameter. It is considered to be due to the release of induced strains or supersaturated solution between Al atoms. On the other hand, a remarkably exothermic heat effect was detected around 503 K in the DTA profile using rapid solidified raw powder as shown in Fig.5. Therefore, the induced strains and supersaturated elements in the matrix of the as-received raw powder are reduced by heating over 503 K. No significant peak of intermetallic compounds is detected in raw powder because of supersaturated solution during the rapid solidification in SWAP. A $MgZn_2$ peak (○) is detected at 573 K, and its intensity decreases with increase in the heat treatment temperature. This result corresponds well with the microstructure changes of intermetallic compounds mentioned in Fig.6. The intensity of Mg_2Si (△) gradually increases at heat treatment temperature over 623 K. The exothermic heat of raw powder at 653 K detected in Fig.5 is due to the precipitation of Mg_2Si. As shown in Fig. 8 (b), 2θof aluminum peak gradually shifts to the lower angle side, that is, the lattice parameter also decreases in the case of the cast ingot alloy. At the same

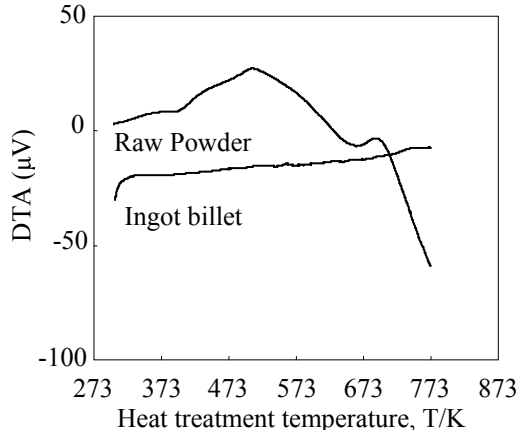

Fig.5 Differential thermal analysis (DTA) of A7075 powder and ingot.

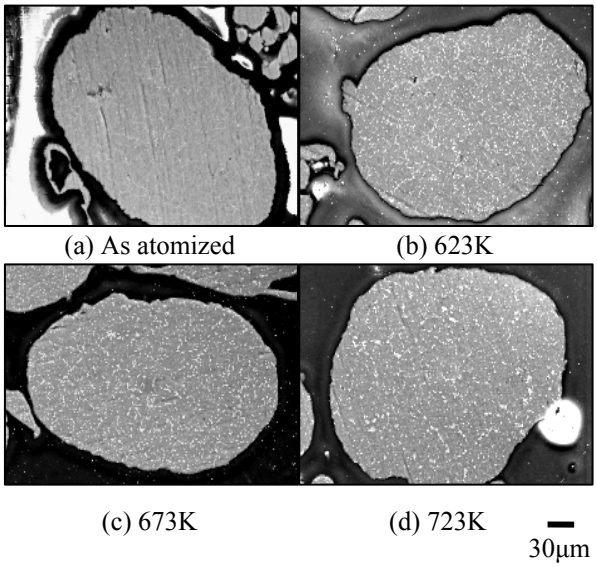

Fig.6 Scanning electron micrographs of as-received A7075 powder and heat-treated ones at various temperatures.

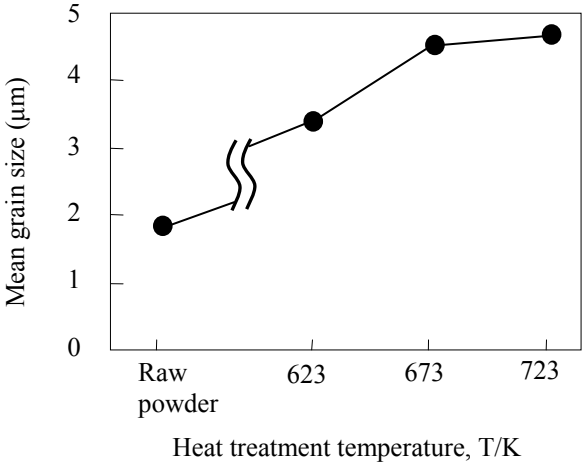

Fig.7 Dependence of mean grain size of A7075 powder on heat treatment temperature.

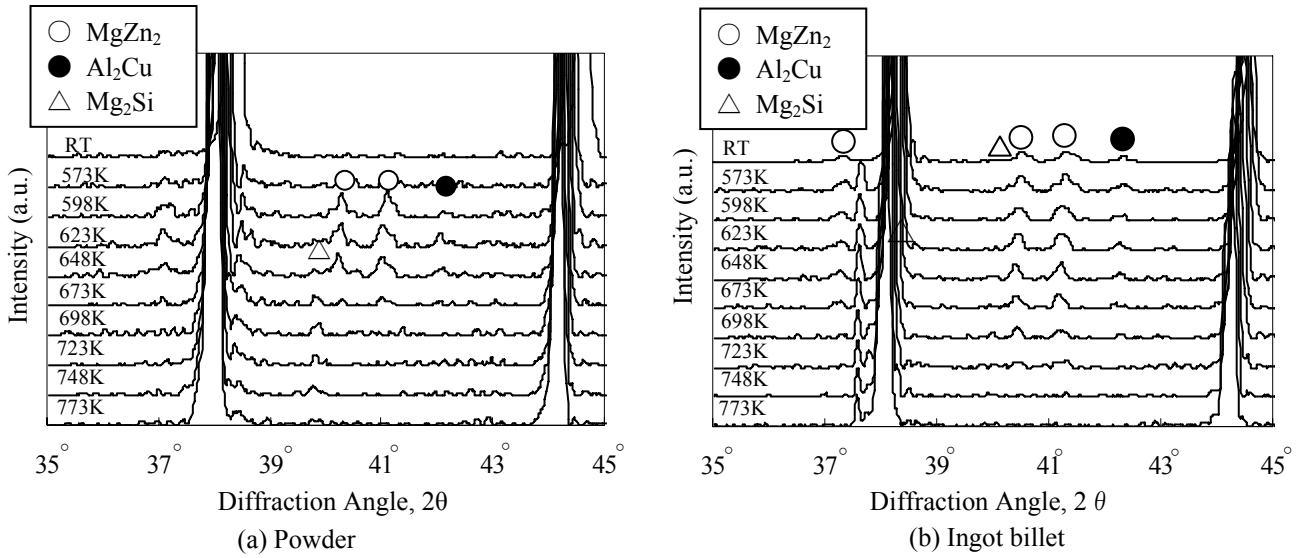

Fig.8 High temperature XRD patterns of A7075 powder and ingot billet at various temperatures.

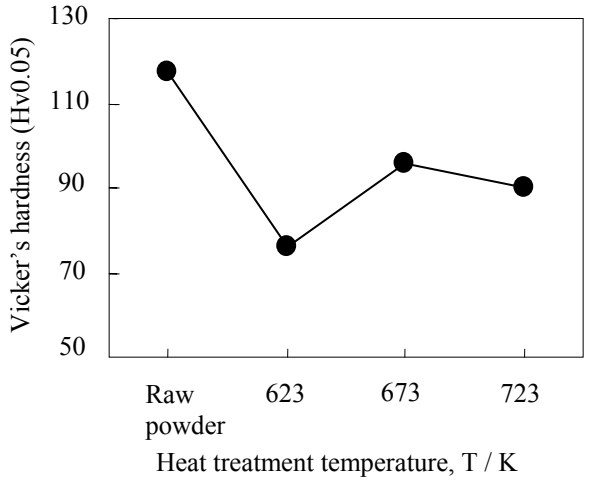

Fig.9 Vicker's hardness of annealed A7075 powder.

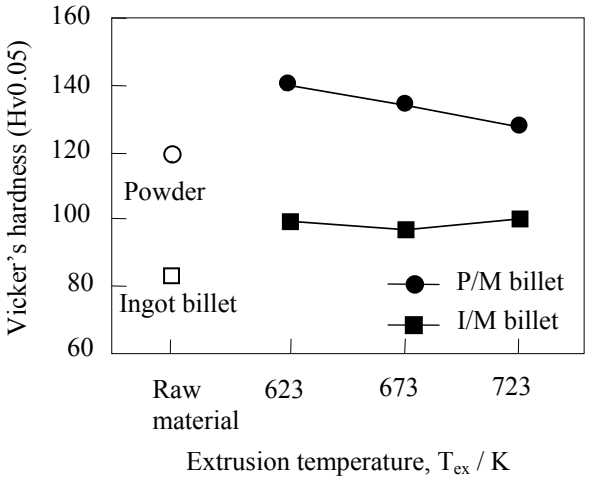

Fig.10 Vicker's hardness of extruded A7075 alloys in using P/M and I/M billets.

time, a decrease of peak intensities of precipitates such as $MgZn_2$, Al_2Cu, and Mg_2Si is detected. Here, the shifting of 2θof aluminum peak is due to the solution of each intermetallic during heating. **Fig.9** shows the dependence of Vicker's hardness of A7075 powder on the heating temperature. Raw powder has a high hardness of 117 Hv because of induced strains and supersaturated metal elements such as Zn, Mg, Cu and Si in the matrix following rapid solidification, as shown in Fig.6 (a) and Fig.8 (a). The hardness of the annealed powder at 623 K decreases to 76 Hv by reducing the strains and grain coarsening. It increases up to 96 Hv again following the precipitation of Mg_2Si at 623~673 K, corresponding to XRD results shown in Fig.8 (a). A small decrease of the hardness at 673~723 K is due mainly to the softening by the solution of $MgZn_2$ precipitates.

3.2 Characteristics of A7075 P/M extruded alloys

Figure 10 shows Vicker's hardness of extruded 7075 alloys for both P/M and I/M billets. The hardness of extruded P/M billets is higher than that of I/M materialsat all extrusion temperatures. The maximum hardness of extruded P/M billet is obtained at the extrusion temperature of 623 K. It gradually decreases with increase in the extrusion temperature from 673 K to 723 K. As mentioned above, in SEM microstructure photos and XRD patterns, the maximum value at 623 K is due to the precipitation of $MgZn_2$ intermetallics and severe plastic deformation in extrusion. On the other hand, the extruded I/M billets reveal no significant dependence of hardness on the extrusion temperature. They also show higher hardness than the ingot billet. This is because of the severe plastic deformation as described above. **Figure 11** shows tensile properties of extruded A7075 alloys by using P/M and I/M billets. Tensile strength (TS) and yield stress (YS) of P/M are superior to the extruded I/M alloys. The maxima are obtained at 623 K. They gradually decrease with increase of extrusion temperature, and this result corresponds to the hardness changes shown in Fig.10. The elongation of P/M materials is lower than

that of I/M ones at all extrusion temperatures. However, P/M has sufficient ductility at 10 % or more. In comparing the fractured surface of tensile test specimens observed by SEM, **Fig.12 (a)** indicates extruded P/M alloys and reveals fine dimple fracture patterns. Furthermore, SEM observation on A7075 alloys extruded at 623 K shows that P/M materials have a mean grain size of 100 nm ~ 1 μm, and that fine intermetallics of Mg_2Si and Al_2Cu are dispersed inside the grains, as shown in **Fig.13 (a)**. On the other hand, in the case of I/M shown in **Fig.12 (b)**, a mean grain size of 500 nm ~ 5μm is observed, and coarse intermetallics exist at the grain boundaries, as shown in **Fig.13 (b)**. Therefore, mechanical properties of extruded P/M billets are superior to those of extruded I/M billets as shown in Fig.11.

4. Conclusion

The effects of the heat treatment temperature before extrusion on microstructures and mechanical properties of A7075 rapidly solidified powder by SWAP and their extruded alloys were investigated. From the obtained results, it can be concluded that;

(1) A supersaturated solid-solution of additive elements is formed during rapid solidification by SWAP. Intermetallic compounds such as $MgZn_2$, Al_2Cu and Mg_2Si are precipitated by heat treatment of the A7075 powder. By increasing the heat treatment temperature, $MgZn_2$ is precipitated from 573 K and dissolved above 673 K, and the coarsening of Mg_2Si is accelerated above 623 K.

(2) High-temperature XRD and Vicker's hardness of A7075 powder have shown that the exothermic heat effect of raw powder at 503 K and 653 K detected in the DTA profile is due to both the strain release and precipitation of Mg_2Si.

(3) A7075 extruded materials via SWAP show fine dimple fractured patterns and mean grain sizes of 100 nm ~ 1 μm with fine intermetallics of Mg_2Si and Al_2Cu dispersed inside the grains and have a good balance of high strength and ductility. For example, when extruding at 623 K A7075 wrought P/M alloys via T5 heat treatment show yield stresses of 370 MPa and elongations of 15 %.

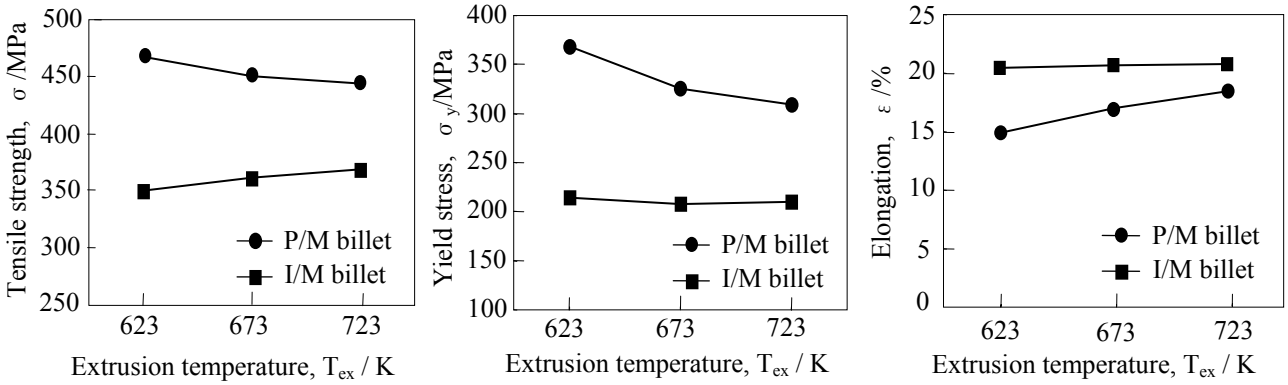

(a) Tensile strength (b) Yield stress (c) Elongation

Fig.11 Tensile properties of extruded A7075 alloys in using P/M and I/M billets.

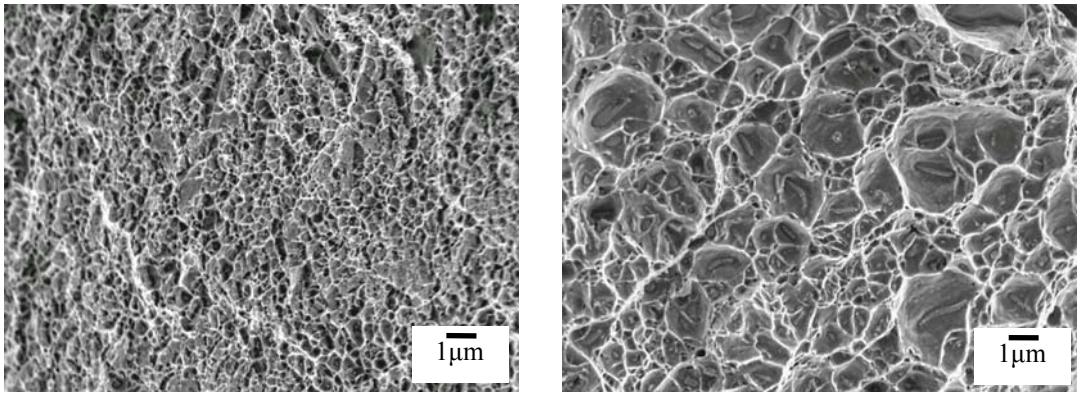

(a) P/M billet (b) I/M billet

Fig.12 Scanning electron micrographs of fractured surfaces in extruded A7075 alloys at 623K in using P/M (a) and I/M billet (b).

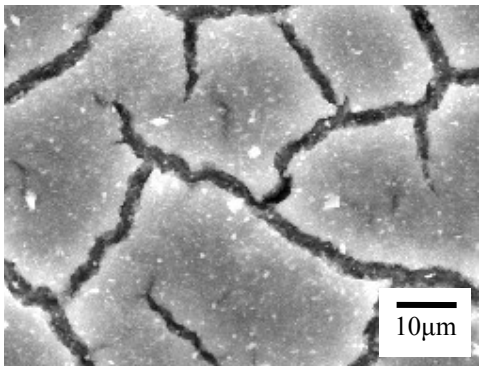

(a) P/M billet

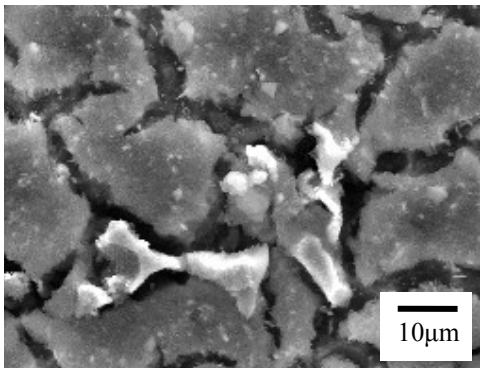

(b) I/M billet

Fig.13 Scanning electron micrographs of extruded A7075 alloys at 623K in using P/M (a) and I/M billet (b).

References

1) Japan Aluminium Association, Aluminum Handbook, vol.6(2001), pp.1-11
2) S. Ishihara, Aluminum Powder Metallurgy Alloys, R&D Review of Toyota CRDL, Vol.30.2(1995), pp.13-22.
3) K. Osamura et al., Effect of Zr Addition on Microstructure of Hot Extruded P/M Al-Zn-Mg-Cu Alloys, Journal of Japan Institute of Light Metals, Vol.55.4(2005), pp.164-168.
4) A. Inoue et al., Preparation of Fe-, Co-, and Ni-Based Amorphous Alloy Powders by High-Pressure Gas Atomization and Their Structural Relaxation Behavior, Metallurgical Transactions A, 19A(1988), pp.235-242.
5) A. V. Krajnikov et al. Surface chemistry of water atomised aluminium alloy powders, Applied Surface Science, Volume 191, Issues 1-4 (2002), pp26-43.
6) Liu-Ho Chiu et al. Comparison between oxide-reduced and water-atomized copper powders used in making sintered wicks of heat pipe, China Particuology, Volume 5, Issue 3(2007) pp220-224.
7) I. Otsuka et al., Production of Amorphous Soft Magnetic Powders by the New Water Atomization Process ”SWAP”, Powder and powder metallurgy, Vol.48.9(2001), pp.697-702.
8) S. Fujino et al., High-Strain-Rate Superplastic Behavior in a Super-Rapidly-solidified Al-Si System Alloy, Scripta Materia, vol.37.5(1997), pp.673-678.